



OPEN ACCESS

EDITED BY

Bo Peng,
Sun Yat-sen University, China

REVIEWED BY

Yin Tang,
University of Southern California,
United States
Syeda Sadia Fatima,
Aga Khan University, Pakistan

*CORRESPONDENCE

Jun Luo
✉ 500210@hospital.cqmu.edu.cn
Dan Jiang
✉ 500218@hospital.cqmu.edu.cn

RECEIVED 15 April 2023

ACCEPTED 23 June 2023

PUBLISHED 19 July 2023

CITATION

Li Y, Feng Y, Yang Z, Zhou Z, Jiang D
and Luo J (2023) Untargeted
metabolomics of saliva in pregnant women
with and without gestational diabetes
mellitus and healthy non-pregnant women.
Front. Cell. Infect. Microbiol. 13:1206462.
doi: 10.3389/fcimb.2023.1206462

COPYRIGHT

© 2023 Li, Feng, Yang, Zhou, Jiang and Luo.
This is an open-access article distributed
under the terms of the [Creative Commons
Attribution License \(CC BY\)](https://creativecommons.org/licenses/by/4.0/). The use,
distribution or reproduction in other
forums is permitted, provided the original
author(s) and the copyright owner(s) are
credited and that the original publication in
this journal is cited, in accordance with
accepted academic practice. No use,
distribution or reproduction is permitted
which does not comply with these terms.

Untargeted metabolomics of saliva in pregnant women with and without gestational diabetes mellitus and healthy non-pregnant women

Yueheng Li^{1,2,3,4}, Yang Feng⁵, Zhengyan Yang^{1,2,3,4}, Zhi Zhou^{1,2,3,4},
Dan Jiang^{1,2,3,4*} and Jun Luo^{1,2,3,4*}

¹Department of Preventive Dentistry, Stomatological Hospital of Chongqing Medical University, Chongqing, China, ²College of Stomatology, Chongqing Medical University, Chongqing, China,

³Chongqing Key Laboratory of Oral Diseases and Biomedical Sciences, Chongqing, China, ⁴Chongqing Municipal Key Laboratory of Oral Biomedical Engineering of Higher Education, Chongqing, China,

⁵Chongqing Changshou Health Center for Women and Children, Chongqing, China

Objective: The aim of this study was to compare the differences in salivary metabolites between pregnant women with gestational diabetes mellitus (GDM), healthy pregnant women (HPW), and healthy non-pregnant women (HNPW), and analyze the possible associations between the identified metabolites and gingivitis.

Method: The study included women with GDM ($n = 9$, mean age 28.9 ± 3.6 years, mean gestational age 30.1 ± 3.2 weeks), HPW ($n = 9$, mean age 27.9 ± 3.0 years, mean gestational age 28.6 ± 4.7 weeks), and HNPW ($n = 9$, mean age 27.7 ± 2.1 years). Saliva samples were collected from all participants and were analyzed with LC-MS/MS-based untargeted metabolomic analysis. Metabolite extraction, qualitative and semi-quantitative analysis, and bioinformatics analysis were performed to identify the differential metabolites and metabolic pathways between groups. The identified differential metabolites were further analyzed in an attempt to explore their possible associations with periodontal health and provide evidence for the prevention and treatment of periodontal inflammation during pregnancy.

Results: In positive ion mode, a total of 2,529 molecular features were detected in all samples, 166 differential metabolites were identified between the GDM and HPW groups (89 upregulated and 77 downregulated), 823 differential metabolites were identified between the GDM and HNPW groups (402 upregulated and 421 downregulated), and 647 differential metabolites were identified between the HPW and HNPW groups (351 upregulated and 296 downregulated). In negative ion mode, 983 metabolites were detected in all samples, 49 differential metabolites were identified between the GDM and HPW groups (29 upregulated and 20 downregulated), 341 differential metabolites were identified between the GDM and HNPW groups (167 upregulated and 174 downregulated), and 245 differential metabolites were identified between the HPW and HNPW groups (112 upregulated and 133 downregulated). A total of nine differential metabolites with high confidence levels were identified in both the

positive and negative ion modes, namely, L-isoleucine, D-glucose 6-phosphate, docosahexaenoic acid, arachidonic acid, adenosine, adenosine-monophosphate, adenosine 5'-monophosphate, xanthine, and hypoxanthine. Among all pathways enriched by the upregulated differential metabolites, the largest number of pathways were enriched by four differential metabolites, adenosine, adenosine 5'-monophosphate, D-glucose 6-phosphate, and adenosine-monophosphate, and among all pathways enriched by the downregulated differential metabolites, the largest number of pathways were enriched by three differential metabolites, L-isoleucine, xanthine, and arachidonic acid.

Conclusion: Untargeted metabolomic analysis of saliva samples from pregnant women with GDM, HPW, and HNPW identified nine differential metabolites with high confidence. The results are similar to findings from previous metabolomics studies of serum and urine samples, which offer the possibility of using saliva for regular noninvasive testing in the population of pregnant women with and without GDM. Meanwhile, the associations between these identified differential metabolites and gingivitis need to be further validated by subsequent studies.

KEYWORDS

gestational diabetes mellitus, pregnant women, saliva, gingivitis, untargeted metabolomics

1 Introduction

It has been proven that periodontal disease is one of the risk factors for adverse pregnancy outcomes in pregnant women (Wu et al., 2015; Komine-Aizawa et al., 2019). Gingivitis is the most prevalent oral disease during pregnancy, which is more likely to occur in the second and third trimester of pregnancy. The gums of patients are hyperemic, swollen, and bleeding. Gingivitis affects 30%–70% of pregnant women worldwide (Dommisch et al., 2015), and the prevalence of pregnancy gingivitis is 60%–90% in China (Hu et al., 1999). Xiong et al. (2006) concluded that the prevalence of periodontitis in women with and without gestational diabetes mellitus (GDM) was 44.8% and 13.2%, respectively, and the results demonstrate a correlation between periodontitis and GDM. Therefore, it is clinically important to effectively prevent or treat periodontal diseases, control periodontitis-associated local and systemic inflammation, maintain oral health, and avoid the occurrence of adverse pregnancy outcomes in pregnant women, especially in pregnant women with GDM.

Saliva is a complex fluid that plays an important role in the maintenance of oral health. Salivary components contain not only a large amount of water, but also various electrolytes, proteins, and a large amount of volatile organic compounds that originate from compounds produced by microorganisms in the oral cavity, such as fatty ammonia, branched-chain fatty acids, indoles, phenols, and volatile sulfur-containing compounds (Cheng et al., 2016). Many blood components enter the saliva via intracellular transport pathways (passive intracellular diffusion and active transport) or

paracellular pathways (extracellular ultrafiltration) (Haeckel and Hnecke, 1993; Jusko and Milsap, 1993). Most compounds found in blood are also present in saliva. Saliva testing can provide insight into the health and disease status of human body.

Untargeted metabolomics is an approach that aims to identify differentially expressed metabolites using univariate and multivariate statistical methods, thus reflecting the internal environment of cells and their interaction with external influencing factors. Goldsmith (Goldsmith et al., 2010) et al. suggest that metabolomics has an important role in clinical diagnosis of diseases. In recent years, a lot of attention has been paid to the basic saliva research; saliva presents an obvious advantage in diagnosing diseases earlier (Cheng et al., 2014; Zhang et al., 2016). Metabolomics full-spectrum analysis is a technique for the identification and quantification of all metabolites in organisms, discovering the relative relationship between metabolites and physiopathological changes, which focuses on small molecules with a relative molecular mass of less than 1,000, such as lipids, ketones, and organic acids.

Therefore, in this study, we conducted untargeted metabolomics on saliva samples from pregnant women with GDM, healthy pregnant women (HPW), and healthy non-pregnant women (HNPW) using liquid chromatography–tandem mass spectrometry (LC-MS/MS) to investigate the differences in salivary metabolites between these patients, and explore their possible associations with gingivitis, in an attempt to identify possible key metabolites and related metabolic pathways, and provide new ideas for the prevention and treatment of GDM and pregnancy gingivitis.

2 Materials and methods

2.1 Saliva samples

Twenty-seven pregnant and non-pregnant women who received preconception health examination and antenatal examination in the Maternal and Child Health Hospital of Changshou District in January 2022 were included, namely, nine pregnant women with GDM (mean age 28.9 ± 3.6 years, mean gestational age 30.1 ± 3.2 weeks, fasting plasma glucose 5.55 ± 0.17 mmol/L), nine HPW (mean age 27.9 ± 3.0 years, mean gestational age 28.6 ± 4.7 weeks, fasting plasma glucose 4.57 ± 0.33 mmol/L), and nine HNPW (mean age 27.7 ± 2.1 years, fasting plasma glucose 4.4 ± 0.085 mmol/L).

This study was approved by the Research Ethics Committee of Stomatological Hospital of Chongqing Medical University.

2.2 Inclusion criteria

Women were included in the GDM group if they were diagnosed with gestational diabetes mellitus (GDM) during antenatal examination by oral glucose tolerance test according to the diagnostic criteria recommended by the International Association of Diabetes and Pregnancy Study Group (IADPSG) in 2011; did not have dental caries; have moderate gingivitis assessed based on the modified Loe–Silness gingival index (presenting as shiny, red, swollen gums that bleed easily upon probing); had no systemic or congenital diseases, developmental malformations, and bacterial or severe infections in other parts of the body; did not take antibiotics, fluorides, and microecological modulators; and did not receive orthodontic treatment within the last 3 months.

Women were included in the HPW group if they did not have blood glucose abnormalities and dental caries; have moderate gingivitis assessed by the modified Loe–Silness gingival index (presenting as shiny, red, swollen gums that bleed easily upon probing); have no systemic or congenital diseases, developmental malformations, and bacterial or severe infections in other parts of the body; did not take antibiotics, fluorides, and microecological modulators; and did not receive orthodontic treatment within the last 3 months.

Women were included in the HNPW group if they did not have dental caries, gingivitis assessed by the modified Loe–Silness gingival index, systemic or congenital diseases, developmental malformations, and bacterial or severe infections in other parts of the body; and did not take antibiotics, fluorides, and microecological modulators, and did not receive orthodontic treatment within the last 3 months.

Patients with a history of chronic disease, diabetes, thyroid function disease, and other metabolic diseases are excluded from this study

2.3 Saliva sample collection

Non-stimulated whole saliva was collected from all participants according to the modified Rhodus method (Rhodus et al., 2005) between 9:00 and 11:00 a.m. All participants fasted 1 h prior to collection. During collection, participants were asked to let saliva

collect in their mouth for at least 1 min and spit into a centrifuge tube or sterile cup; it is not allowed to spit sputum. This process needs to be repeated several times in order to ensure that an adequate volume (2–5 ml) of saliva was collected. The collected saliva samples were placed in an ice box and transported immediately to the laboratory. After centrifugation at 5,000g at 4°C for 10 min, the supernatant was collected and filtered through a 0.22- μ m sterile membrane; 1 ml was dispensed into labeled 2-ml Eppendorf tubes and stored at -80°C . Before undertaking untargeted metabolomic analysis, all samples were taken and thawed.

Extraction and preparation steps of saliva metabolites: ① Add 100 μ l of each sample into the corresponding centrifuge tube, and freeze the remaining samples. ② Add 700 μ l of the extractant containing internal standard 1 (methanol:acetonitrile:water = 4:2:1), shake for 10 min, and place it in a refrigerator at -20°C for 2 h. ③ Centrifuge at 25,000g at 4°C for 15 min. ④ The sample is removed from the centrifuge and 600 μ l of supernatant is transferred to a new centrifuge tube. ⑤ Drain with a drainer. ⑥ Add 180 μ l of methanol:pure water (1:1 v/v) and swirl for 10 min until it is completely dissolved in the complex solution. ⑦ Centrifuge at 25,000g at 4°C for 15 min again. ⑧ The remaining samples (50 μ l each) were taken into the three upper plates for the detection of positive and negative ions, and the other plate was used as the spare plate, and the remaining samples (20 μ l mixed QC) were taken.

2.4 Untargeted metabolomic analysis of saliva samples

Untargeted metabolomic analysis of saliva samples from women with GDM, HPW, and HNPW was performed using the LC-MS/MS method. A high-resolution mass spectrometer, Q Exactive (Thermo Fisher Scientific, USA), was used to collect data in both the positive and negative ion modes in order to improve the coverage of metabolites. The raw data generated by LC-MS/MS were processed using Compound Discoverer 3.1 software (Thermo Fisher Scientific, USA) to perform peak alignment, peak picking, and compound identification.

2.5 Statistical analysis

Data pre-processing, statistical analysis, and metabolite taxonomic and functional annotations were performed using the metabolomics R software package metaX (Wen et al., 2017) and the metabolome information analysis process. Principal component analysis (PCA) was used to reduce the dimensionality of original multivariate data to analyze the groupings, trends (similarities and differences within and between sample groups), and outliers (presence of outlier samples) of the observed variables in the data set. The variable importance in the projection (VIP) values of the first two principal components of the partial least squares discriminant analysis (PLS-DA) model (Barker and Rayens, 2003; Westerhuis et al., 2008) combined with the multiplicity of variance change (fold change) obtained from the univariate analysis and the *t*-test (Student's *t*-test) results were used to screen for differential metabolites.

In a strict sense, biological data did not strictly obey normal distribution. Before *t*-test, we processed the data by log2 to make the data approximately obey normal distribution, so that the result of *t*-test is relatively more reasonable. At the same time, considering that the difference between groups is not so significant, we used *p*-value (Zheng et al., 2019) as the condition for screening the difference in order to screen the appropriate differential metabolites for subsequent research and did not correct it.

3 Saliva metabolomics results

3.1 Results of sample quality control

As shown in Figures 1A, B, after overlapping the base peak ion chromatograms of all quality control samples, the chromatograms well overlapped in both the positive and negative ion modes, the retention time and peak response intensity fluctuated little, indicating that the instrument was in a good state with stable

signal during the whole sample detection process. A PCA analysis of the QC sample and all samples can be used to observe the overall distribution of each set of samples and the stability of the entire analytical process. As shown in Figures 1C, D, the better the QC samples aggregate, the more stable the instrument and the better the repeatability of the acquired data. CV distribution of compounds in each sample as shown in Figures 1E, F.

3.2 Results of compound identification

The results of this study showed that in positive ion mode, a total of 2,529 metabolites were detected in all saliva samples; 905 out of these 2,529 metabolites could be found in the Chemspider and mzCloud databases with corresponding compound information. In negative ion mode, a total of 983 metabolites were detected in all saliva samples, 335 out of these metabolites could be found in the Chemspider and mzCloud databases with corresponding compound information Table 1.

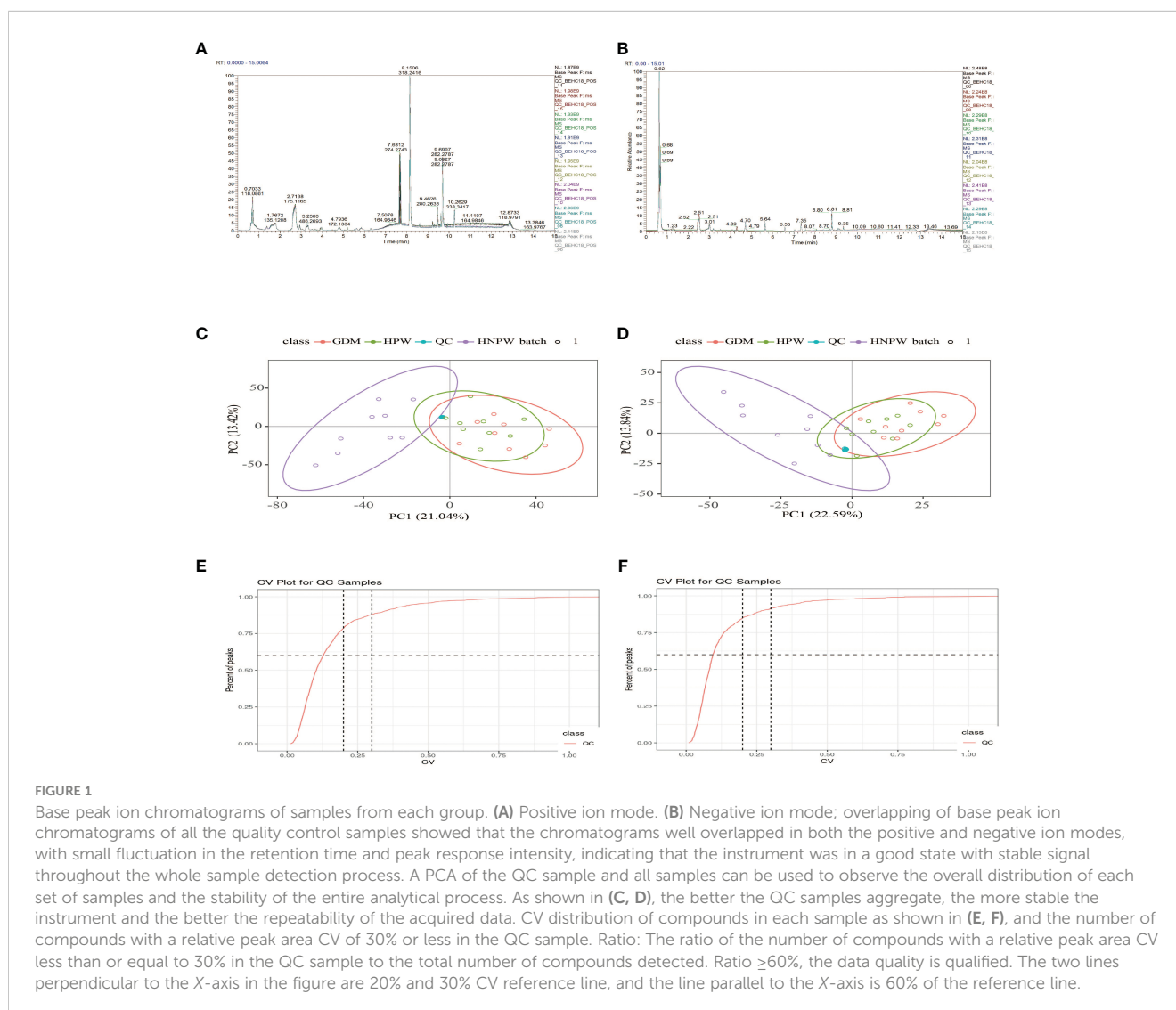


TABLE 1 Number of compounds and number of compounds with identification information identified in positive and negative ion modes.

| Mode | Number of compounds | Number of compounds with identification information |
|-------------------------|---------------------|---|
| Positive ion mode (pos) | 2,529 | 905 |
| Negative ion mode (neg) | 983 | 335 |

Positive ion mode (pos): when the substances are ionized in an ion source, the adduct ions are positive ions, such as H⁺, NH₄⁺, Na⁺, and K⁺.

Negative ion mode (neg): when the substances are ionized in an ion source, the adduct ions are negative ions, such as -H, +Cl.

3.3 Classification of metabolites

The identified metabolites were annotated using the Kyoto Encyclopedia of Genes and Genomes (KEGG) database and Human Metabolome Database (HMDB) to understand the classification of metabolites. The number of metabolites in each class is shown in Figures 2A, B. Identification results without classification information were not included in the analysis. At the same time, the identified metabolites were functionally annotated by the KEGG database in order to understand their functional properties, and determine the major biochemical

metabolic pathways and signal transduction pathways involved in the metabolites. The number of metabolites identified in each type of metabolic pathways is shown Figures 2C, D.

3.4 Statistical analysis

By comparing among groups in the positive ion mode, a total of 166 differential metabolites were identified between the GDM and HPW groups, of which 89 were upregulated and 77 were downregulated; a total of 823 differential metabolites were identified between the GDM and HNPW groups, of which 402 were upregulated and 421 were downregulated; a total of 647 differential metabolites were identified between the HPW and HNPW groups, of which 351 were upregulated and 296 were downregulated in the positive ion mode. In the negative ion mode, a total of 49 differential metabolites were identified between the GDM and HPW groups, of which 29 were upregulated and 20 were downregulated; a total of 341 differential metabolites were identified between the GDM and HNPW groups, of which 167 were upregulated and 174 were downregulated; a total of 245 differential metabolites were identified between the HPW and HNPW groups, of which 112 were upregulated and 133 were downregulated Figure 3.

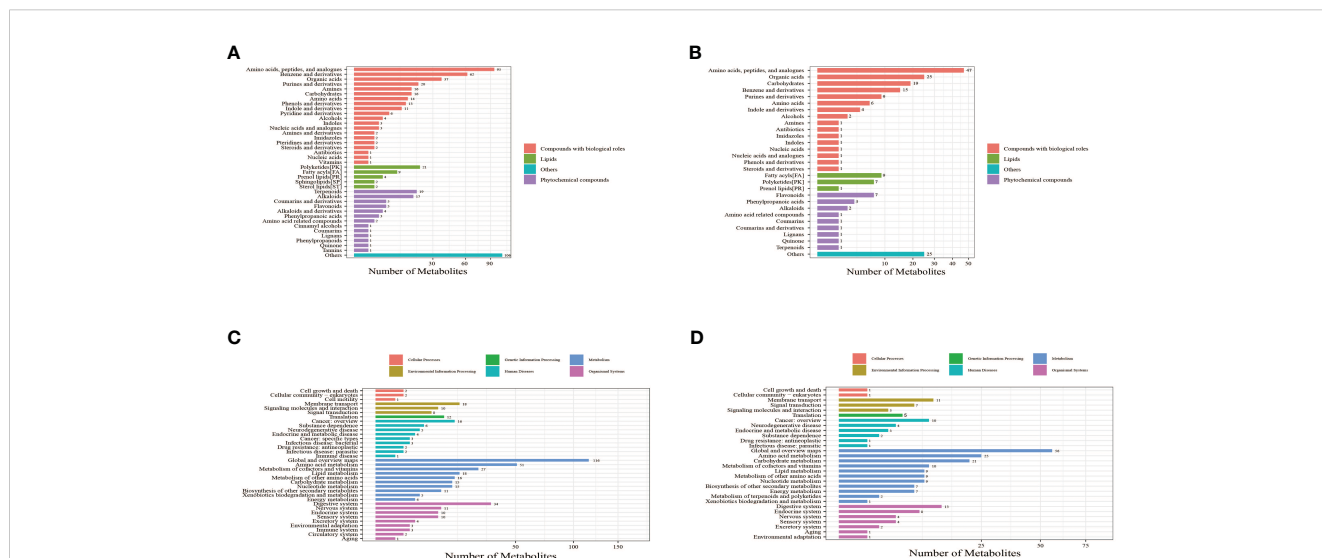


FIGURE 2

Bar chart of metabolite classification in positive ion mode (A) and negative ion mode (B). The X-axis represents the number of metabolites in each class, and the Y-axis represents the metabolite classification entries. Others mean that classification information is the remaining category. The results showed that among the 905 molecular features identified in the positive ion mode, 515 molecular features were classified into four categories, including compounds with biological roles ($n = 311$), lipids ($n = 38$), phytochemical compounds ($n = 61$), and others ($n = 105$). Among the 335 metabolites identified in the negative ion mode, 126 molecular features were classified into four categories, including compounds with biological roles ($n = 195$), lipids ($n = 17$), phytochemical compounds ($n = 18$), and others ($n = 25$). Bar chart of KEGG functional annotation of metabolites in positive ion mode (C) and negative ion mode (D). The X-axis represents the number of metabolites, and the Y-axis represents KEGG pathway entries. The results showed that in positive ion mode, 34 KEGG pathways involving 451 metabolites were annotated. The top four pathways with the largest number of metabolites were global and overview maps (116 metabolites), amino acid metabolism (51 metabolites), digestive system (34 metabolites), and metabolism of cofactors and vitamins (27 metabolites). The number of metabolites contained in these four pathways accounted for 50.55% of all metabolites annotated to the pathways. In negative ion mode, 30 KEGG pathways involving 238 metabolites were annotated. The top four pathways with the largest number of metabolites were global and overview maps (56 metabolites), amino acid metabolism (25 metabolites), carbohydrate metabolism (21 metabolites), and digestive system (13 metabolites). The number of metabolites contained in these four pathways accounted for 48.32% of all metabolites annotated to the pathways. These results suggest that metabolites with identification information detected and identified in either the positive or negative ion modes functioned mainly through two types of KEGG pathways, metabolism and organismal systems.

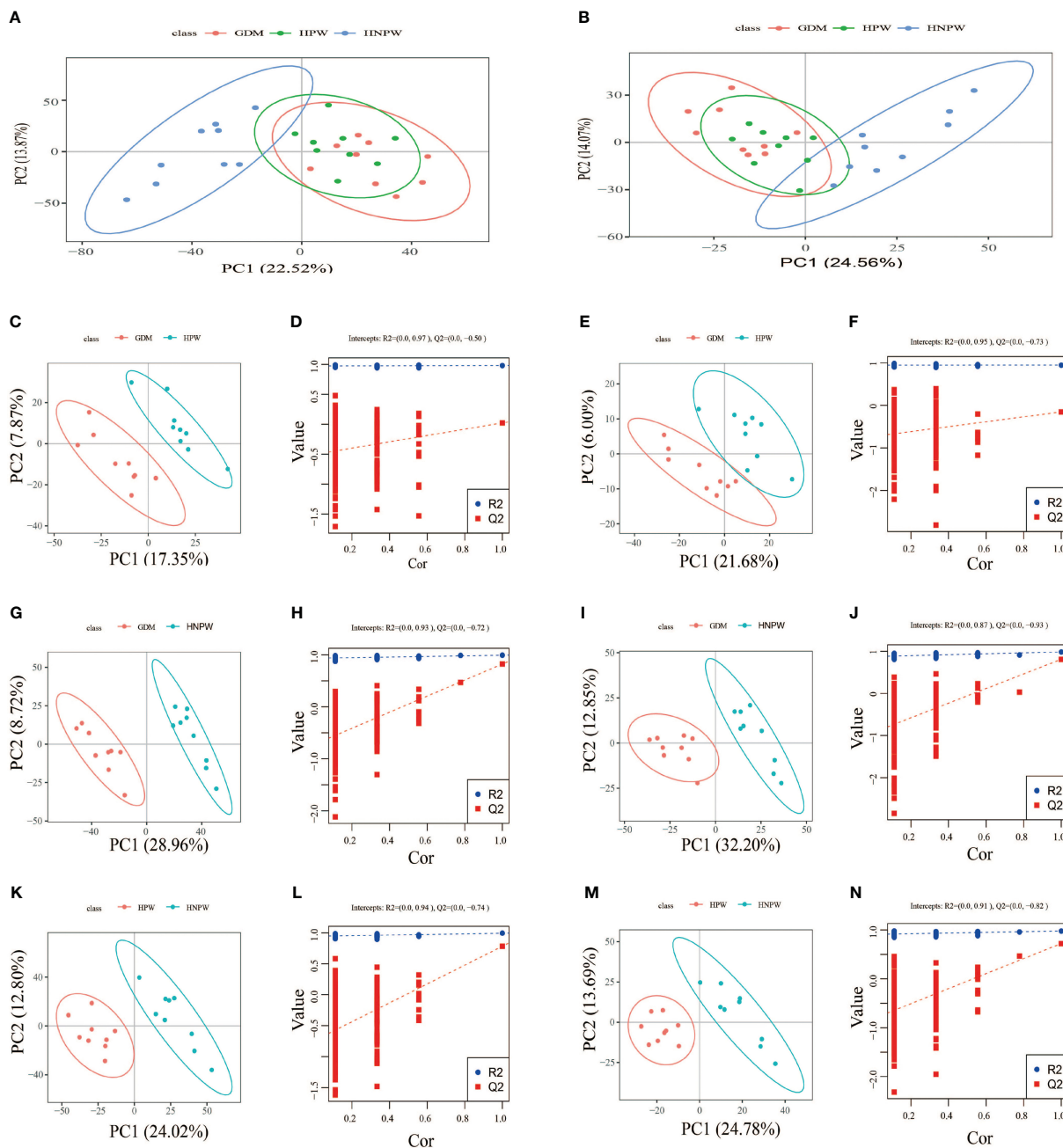


FIGURE 3

(A, C, D, G, H, K, L) Positive ion mode. (B, E, F, I, J, M, N) Negative ion mode. GDM, gestational diabetes mellitus; HPW, healthy pregnant women; HNPW, healthy non-pregnant women. A PCA model was constructed to observe the distribution and separation of samples between the groups. Data were log transformed (log2) prior to constructing PCA mode and scaled using the Pareto scaling method. PCA results. (A, B) The abscissa is the first principal component PC1, the ordinate is the second principal component PC2, and the ellipse in the PCA score graph is 95% confidence interval. Each dot represents a sample, and different groups are labeled with different colors. The number is the score of the principal component, which represents the percentage of the explanation on overall variance of the specific principal component. PLS-DA results. PLS-DA score plots between gestational diabetes mellitus (GDM) and healthy pregnant women (HPW) groups in positive (C) and negative ion modes (E). PLS-DA score plots between the GDM group and the healthy non-pregnant women (HNPW) group in positive (G) and negative ion modes (I). PLS-DA score plots between the HPW group and the HNPW group in positive (K) and negative ion modes (M). The horizontal axis represents the first principal component; the vertical axis represents the second principal component. The number in parentheses is the score of the principal component, which represents the percentage of the overall variance explained by the corresponding principal component. Based on the following conditions, (1) the VIP of the first two principal components of the PLS-DA model ≥ 1 ; (2) fold-change ≥ 1.2 or ≤ 0.83 ; and (3) p -value < 0.05 , the differential metabolites among groups were identified (Table 2). The two rightmost points in the figure are the actual R2 and Q2 values of the PLS-DA model, and the remaining points are the R2 and Q2 values obtained by randomly arranging the samples used (D, F, H, J, L, N).

3.5 Results from volcano plot and metabolic pathway enrichment analysis of differential metabolites

Metabolic pathway enrichment analysis was performed based on the KEGG database **Figure 4**. Metabolic pathways with a p -value < 0.05 were considered to be significantly enriched by differential metabolites. The X-axis shows the enrichment factor. A larger enrichment factor indicates a greater degree of enrichment. The size of dots represents the number of differential metabolites annotated to the pathway. The dot size represents the number of differential metabolites annotated to this pathway. Enrichment analysis was based on annotated metabolites in the KEGG database. The annotation results of differentiated metabolites screened in this project were statistically analyzed by combining the hypergeometric test, and the p -value of corresponding pathway was obtained. Then, p -value < 0.05 was taken as the threshold to determine whether the pathway was enriched or not. The ggplot2 package in the R package is used for mapping.

In the present study, metabolic pathway enrichment analysis results of differential metabolites between GDM and HPW groups

showed that in positive ion mode (**Figure 4B**), six enriched metabolic pathways were significantly different between the two groups, namely, alpha-linolenic acid metabolism [enriched by two metabolites 12-oxo phytodienoic acid and 13(s)-HOTrE]; valine, leucine, and isoleucine biosynthesis (enriched by L-isoleucine); carbohydrate digestion and absorption (enriched by sucrose); mineral absorption (enriched by L-isoleucine); ABC transporters (enriched by sucrose and L-isoleucine); and metabolic pathway [enriched by sucrose, hypoxanthine, L-isoleucine, dihydroxyindole, (+/-)-tropinone, bisphenol A, 12-oxo phytodienoic acid, and protoporphyrin IX]. In negative ion mode (**Figure 4D**), five enriched metabolic pathways were significantly different between the two groups, including caffeine metabolism (enriched by xanthine), carbohydrate digestion and absorption (enriched by maltotriose), and biosynthesis of unsaturated fatty acids (enriched by docosahexaenoic acid), purine metabolism (enriched by xanthine), and ABC transporters (enriched by maltotriose). Among the six differential metabolic pathways in positive ion mode, four differential pathways were enriched with L-isoleucine and three were enriched with sucrose. Among the five differential

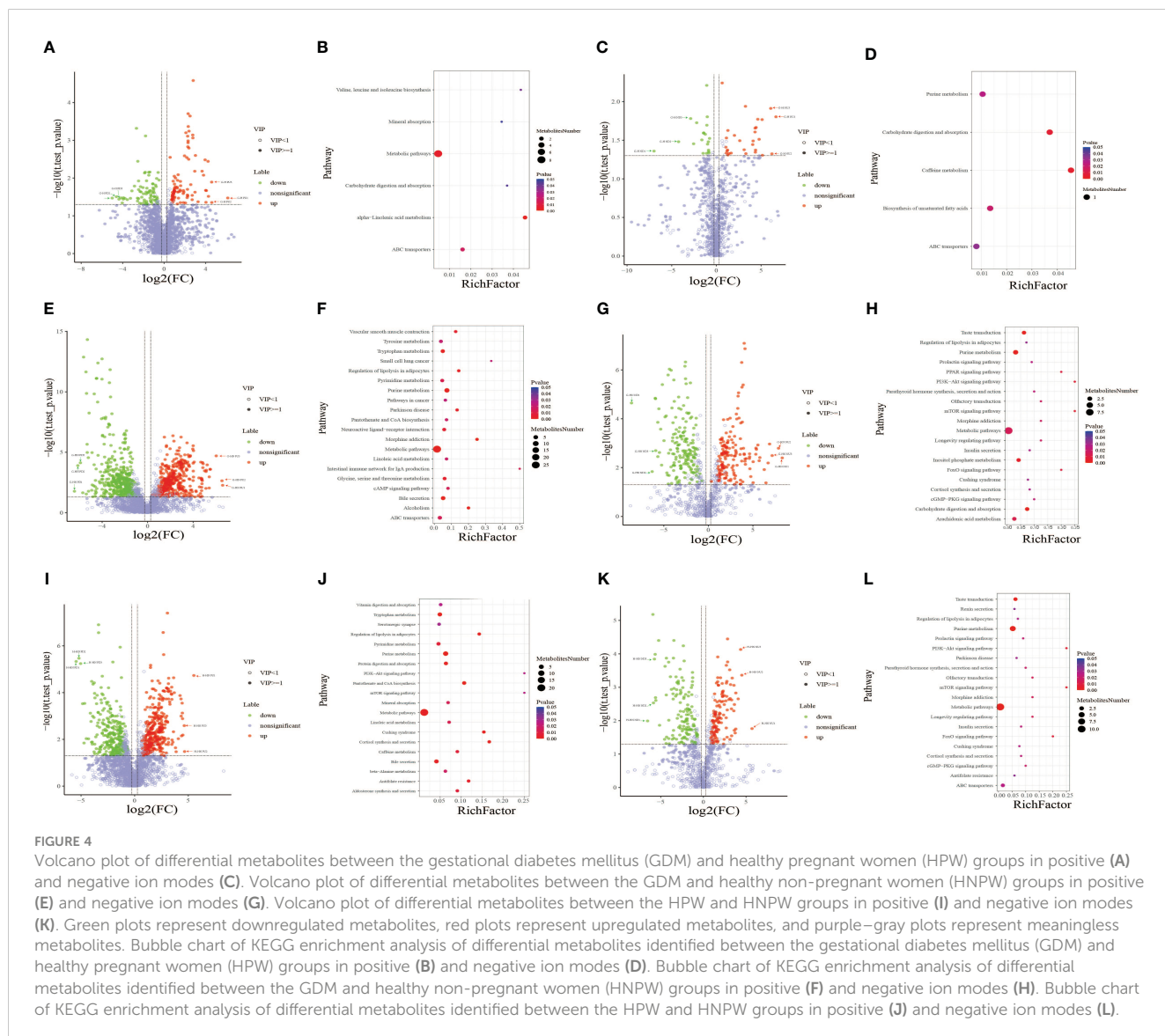


FIGURE 4

Volcano plot of differential metabolites between the gestational diabetes mellitus (GDM) and healthy pregnant women (HPW) groups in positive (A) and negative ion modes (C). Volcano plot of differential metabolites between the GDM and healthy non-pregnant women (HNPW) groups in positive (E) and negative ion modes (G). Volcano plot of differential metabolites between the HPW and HNPW groups in positive (I) and negative ion modes (K). Green plots represent downregulated metabolites, red plots represent upregulated metabolites, and purple-gray plots represent meaningless metabolites. Bubble chart of KEGG enrichment analysis of differential metabolites identified between the gestational diabetes mellitus (GDM) and healthy pregnant women (HPW) groups in positive (B) and negative ion modes (D). Bubble chart of KEGG enrichment analysis of differential metabolites identified between the GDM and healthy non-pregnant women (HNPW) groups in positive (F) and negative ion modes (H). Bubble chart of KEGG enrichment analysis of differential metabolites identified between the HPW and HNPW groups in positive (J) and negative ion modes (L).

TABLE 2 Differential metabolites among groups in positive and negative ion modes.

| Group | Total number of differential metabolites | Number of up- and downregulated metabolites | Expression status | Number of metabolites with different confidence levels | | | | |
|-----------------------------------|--|---|-------------------|--|---------|---------|---------|---------|
| | | | | Level 1 | Level 2 | Level 3 | Level 4 | Level 5 |
| GDM vs. HPW in negative ion mode | 49 | 29 | Up | 0 | 2 | 1 | 6 | 20 |
| | | 20 | Down | 1 | 1 | 1 | 4 | 13 |
| GDM vs. HPW in positive ion mode | 166 | 89 | Up | 1 | 1 | 3 | 27 | 57 |
| | | 77 | Down | 2 | 1 | 0 | 34 | 40 |
| GDM vs. HNPW in negative ion mode | 341 | 167 | Up | 4 | 6 | 0 | 43 | 115 |
| | | 174 | Down | 0 | 6 | 1 | 36 | 131 |
| GDM vs. HNPW in positive ion mode | 823 | 402 | Up | 5 | 9 | 10 | 119 | 259 |
| | | 421 | Down | 0 | 5 | 6 | 143 | 267 |
| HPW vs. HNPW in negative ion mode | 245 | 112 | Up | 8 | 5 | 1 | 68 | 30 |
| | | 133 | Down | 0 | 6 | 0 | 26 | 101 |
| HPW vs. HNPW in positive ion mode | 647 | 351 | Up | 7 | 10 | 7 | 96 | 231 |
| | | 296 | Down | 0 | 3 | 4 | 109 | 180 |

metabolic pathways in negative ion mode, two differential pathways were enriched with xanthine and two were enriched with maltotriose.

The results from metabolic pathway enrichment analysis of differential metabolites between GDM and HNPW groups showed that in positive ion mode (Figure 4F), 27 enriched metabolic pathways were significantly different between the two groups; the top three metabolic pathways with the largest differences between the two groups were intestinal immune network for IgA production (enriched with retinoate), small cell lung cancer (enriched with retinoate), and morphine addiction (enriched with two metabolites adenosine and dopamine). In negative ion mode (Figure 4H), 28 enriched metabolic pathways were significantly different between the two groups, and the top three differential metabolic pathways were mTOR and PI3K-Akt signaling pathways, FoxO and PPAR signaling pathways, and olfactory transduction, morphine addiction, and longevity regulating pathway; except for the PPAR signaling pathway that was enriched by 8(s)-hydroxy-(5z,9e,11z,14z)-eicosatetraenoic acid, the remaining pathways were enriched by adenosine 5'-monophosphate. Among the 29 differential metabolic pathways in the positive ionization mode, the largest number of metabolic pathways were enriched by the four differential metabolites adenosine, dopamine, arachidonic acid, and retinoate; these four metabolites were enriched in nine, eight, eight, and seven metabolic pathways, respectively. Among the 28 differential metabolic pathways in negative ion mode, the largest number of metabolic pathways were enriched by adenosine 5'-monophosphate and D-glucose 6-phosphate; these two metabolites were enriched in 19 and 7 metabolic pathways, respectively.

Metabolic pathway enrichment analysis results of differential metabolites between HPW and HNPW groups showed that in positive ion mode (Figure 4J), 27 enriched metabolic pathways were significantly different between the two groups; the top three metabolic pathways with the largest differences between the two groups were

PI3K-Akt and mTOR signaling pathways, cortisol synthesis and secretion, and Cushing syndrome. Among these pathways, PI3K-Akt and mTOR signaling pathways were enriched by the differential metabolite adenosine-monophosphate, and the remaining pathways were enriched by adenosine-monophosphate and cortisol. In negative ion mode (Figure 4L), 27 enriched metabolic pathways were significantly different between the two groups; the top three differential metabolic pathways were PI3K-Akt and mTOR signaling pathways, FoxO signaling pathway, and olfactory transduction, morphine addiction, and longevity regulating pathway; these differential pathways were enriched by adenosine 5'-monophosphate. Among the 27 differential metabolic pathways in positive ion mode, the largest number of metabolic pathways were enriched by the five differential metabolites adenosine-monophosphate, arachidonic acid, L-threonine, L-methionine, and cortisol; these five metabolites were enriched in 10, 7, 6, 5, and 5 pathways, respectively. Among the 27 differential metabolic pathways in negative ion mode, the largest number of metabolic pathways were enriched by two differential metabolites, adenosine 5'-monophosphate and D-glucose 6-phosphate, which were involved in 20 and 5 pathways, respectively.

The results (Tables 3–5) showed that among the top three upregulated differential metabolites, only one metabolite with molecular formula $C_{18}H_{17}ClN_2O_6S_2$ that can be found in ChemSpider and mzCloud databases (ID 187436) was classified into others, and belonged to the class of benzodioxoles, but this metabolite was not annotated to a pathway. Among the top three downregulated differential metabolites, one metabolite with molecular formula $C_{17}H_{22}O_5$ that can be found in ChemSpider and mzCloud databases (ID 37260) was classified into phytochemical compounds, and belonged to the class of terpenoids; one metabolite (ChemSpider ID and mzCloud ID: 37260, molecular formula $C_{16}H_{19}NO$) was classified as benzene and derivatives, and had compounds with biological roles; and one metabolite (ChemSpider ID and mzCloud ID: 12665,

TABLE 3 Top 3 (pu1–pu3) upregulated and top 3 (pd1–pd3) downregulated differential metabolites between the gestational diabetes mellitus and healthy pregnant women groups in positive ion mode.

| | Molecular formula | Molecular weight | Level | Family | Metabolites |
|---------|---|------------------|---------|---------------|-------------------------|
| D-P pu1 | C ₁₂ H ₂₅ NO ₁₁ | 359.142 Da | Level 5 | – | – |
| D-P pu2 | C ₁₈ H ₁ ClN ₂ O ₆ S ₂ | 454.0046 Da | Level 4 | Benzodioxoles | Other |
| D-P pu3 | – | 159.0301 Da | Level 5 | – | – |
| D-P pd1 | C ₁₃ H ₂₂ N ₆ O ₃ | 310.1756 Da | Level 5 | – | – |
| D-P pd2 | C ₁₉ H ₂₉ N ₅ O ₂ | 359.2308 Da | Level 4 | – | – |
| D-P pd3 | C ₁₇ H ₂₂ O ₅ | 306.1467 Da | Level 4 | Terpenoids | Phytochemical compounds |

TABLE 4 Top 3 (pu1–pu3) upregulated and top 3 (pd1–pd3) downregulated differential metabolites between the gestational diabetes mellitus and healthy non-pregnant women groups in positive ion mode.

| | ChemSpider ID mzCloud | Molecular formula | Molecular weight | Level | Family | Metabolites |
|---------|--------------------------|---|------------------|---------|-------------------------|---------------------------------|
| D-W pu1 | – | – | 220.0349 Da | Level 5 | – | – |
| D-W pu2 | – | – | 379.0877 Da | Level 5 | – | – |
| D-W pu3 | – | – | 261.0616 Da | Level 5 | – | – |
| D-W pd1 | 12665 | C ₉ H ₁₇ NO | 155.1312 Da | Level 4 | Piperidinones | Others |
| D-W pd2 | 37260 | C ₁₆ H ₁₉ NO | 241.1467 Da | Level 4 | Benzene and derivatives | Compounds with biological roles |
| D-W pd3 | 59352 | C ₃₃ H ₃₄ N ₄ O ₆ | 582.2484 Da | Level 4 | – | – |

molecular formula C₉H₁₇NO) was classified into others, and belonged to the class of piperidinones; these 3 metabolites were also not annotated to specific metabolic pathways. The results (Tables 6–8) showed that among the top three upregulated metabolites, only one metabolite (ChemSpider ID and mzCloud ID:30778505, molecular formula C₉H₇NO₅S) was classified as indole and derivatives, had compounds with biological roles, and was not annotated to specific pathways. Among the top three downregulated metabolites, one metabolite with molecular formula C₁₅H₂₉NO₃ (ChemSpider ID mzCloud code 21513291) and one metabolite with molecular formula C₁₂H₁₁NO₅ (ChemSpider ID mzCloud code 74852585) were classified as amino acids, peptides, and analogues, and had compounds with biological roles, which were not annotated to specific metabolic pathways Table 9.

3.6 Metabolic pathway enrichment analysis results of differential metabolites with identification confidence levels 1 and 2 between different groups

Table 9 presents the specific information of each differential metabolite with confidence levels 1 and 2, after conducting pathway enrichment analysis of (GDM vs. HPW), (GDM vs. HNPW), and (HPW vs. HNPW) differential metabolites.

4 Discussion

In the present study, nine samples were included in each group. Based on our previous study on oral microbial diversity of dental

TABLE 5 Top 3 (pu1–pu3) upregulated and top 3 (pd1–pd3) downregulated differential metabolites between the healthy pregnant women and healthy non-pregnant women groups in positive ion mode.

| | ChemSpider ID mzCloud | Molecular formula | Molecular weight | Level | Family | Metabolites |
|---------|--------------------------|--|------------------|---------|--------|-------------|
| P-W pu1 | – | C ₇ H ₁₂ N ₅ O ₄ P | 261.0616 Da | Level 5 | – | – |
| P-W pu2 | 29738718 | C ₂₄ H ₁₉ FN ₂ O ₃ | 402.1362 Da | Level 4 | – | – |
| P-W pu3 | – | C ₁₀ H ₂₂ NO ₁₂ P | 379.0877 Da | Level 5 | – | – |
| P-W pd1 | – | C ₂₆ H ₄₆ N ₆ O ₉ | 586.3327 Da | Level 5 | – | – |
| P-W pd2 | 6001 | C ₁₇ H ₁₂ I ₂ O ₃ | 517.8899 Da | Level 4 | – | – |
| P-W pd3 | 7826270 | C ₂₇ H ₃₂ F ₆ O ₃ | 518.2244 Da | Level 4 | – | – |

TABLE 6 Top 3 (pu1–pu3) upregulated and top 3 (pd1–pd3) downregulated differential metabolites between the gestational diabetes mellitus and healthy pregnant women groups in negative ion mode.

| | ChemSpider ID mzCloud | Molecular formula | Molecular weight | Level | Family | Metabolites |
|------------|--------------------------|---|---------------------|------------|---|------------------------------------|
| D-P nu1 | – | C ₁₄ H ₁₉ N ₅ O ₇ S | 401.0987 Da | Level 5 | – | – |
| D-P nu2 | – | C ₁₆ H ₂₄ N ₄ O ₁₀ | 432.1473 Da | Level 5 | – | – |
| D-P nu3 | – | C ₃₄ H ₆₂ N ₆ O ₈ | 682.4654 Da | Level 5 | – | – |
| D-P nd1 | 21513291 | C ₁₅ H ₂₉ NO ₃ | 271.2142 Da | Level 4 | Amino acids, peptides, and analogues | Compounds with biological roles |
| D-P nd2 | – | C ₆ H ₅ C ₇ O ₃ S | 191.9647 Da | Level 5 | – | – |
| D-P nd3 | 74852585 | C ₁₂ H ₁₁ NO ₅ | 249.0633 Da | Level 4 | Amino acids, peptides, and analogues | Compounds with biological roles |

plaque and salivary samples from nine pregnant women with GDM, nine HPW, and nine HNPW, at both species and genus levels, species accumulation curves showed that when the sample size reached nine per group, the number of new species in different oral environments would not significantly increase with an increasing sample size, there is a tendency toward saturation in species richness, and all currently recognized pathogenic bacteria associated with periodontal diseases have been detected. Therefore, in the present study, we considered a sample size of nine for each group, and performed untargeted metabolomic analysis to identify salivary metabolites that were differentially expressed in the saliva of women with GDM, HPW, and HNPW, and explore the possible correlation between the identified differential salivary metabolites and periodontal health.

The combination of three dimensions, retention time, and MS1 and MS2 spectra, is currently the most widely used approach to improve the confidence of metabolite identification in metabolomic analysis (Liang et al., 2020; Shen et al., 2020). In terms of confidence

levels of metabolites identified in the present study, among the top three upregulated and top three downregulated differential metabolites identified in both the positive and negative ion modes (36 metabolites), 14 metabolites were identified with identification confidence level 4 and 22 were identified with identification confidence level 5. It can be seen that although a variety of differential metabolites were identified, relatively few metabolites with high confidence were available for further analysis, and their biological information needs to be further explored and analyzed.

Furthermore, we can see that although the metabolic pathway is enriched by the largest number of differential metabolites, the pathway showed little difference between groups.

Branched-chain amino acids (BCAAs) are essential amino acids, including leucine, isoleucine, and valine, which cannot be synthesized by the human body itself. The levels of BCAAs in plasma are associated with diabetes. The results of this study showed that compared with the HNPW group, the level of isoleucine was decreased in the GDM group, and increased in the

TABLE 7 Top 3 (pu1–pu3) upregulated and top 3 (pd1–pd3) downregulated differential metabolites between the gestational diabetes mellitus and healthy non-pregnant women groups in negative ion mode.

| | ChemSpider ID mzCloud | Molecular formula | Molecular weight | Level | Family | Metabolites |
|------------|--------------------------|--|---------------------|------------|---|------------------------------------|
| D-W nu1 | 30778505 | C ₉ H ₇ NO ₅ S | 241.0042 Da | Level 4 | Indole and derivatives | Compounds with biological roles |
| D-W nu2 | – | C ₇ H ₄ N ₂ O ₄ S | 211.989 Da | Level 5 | – | – |
| D-W nu3 | – | C ₂₀ H ₃₇ N ₃ O ₁₀ | 479.2471 Da | Level 5 | – | – |
| D-W nd1 | 74852585 | C ₁₂ H ₁₁ NO ₅ | 249.0633 Da | Level 4 | Amino acids, peptides, and analogues | Compounds with biological roles |
| D-W nd2 | – | C ₄₆ H ₇₅ N ₄ O ₁₆ P | 970.4906 Da | Level 5 | – | – |
| D-W nd3 | – | C ₂₃ H ₄₁ N ₅ O ₇ | 499.2996 Da | Level 5 | – | – |

TABLE 8 Top 3 (pu1–pu3) upregulated and top 3 (pd1–pd3) downregulated differential metabolites between the healthy pregnant women and healthy non-pregnant women groups in negative ion mode.

| | ChemSpider ID mzCloud | Molecular formula | Molecular weight | Level | Family | Metabolites |
|---------|--------------------------|--|------------------|---------|--------|-------------|
| P-W nu1 | – | C ₇ H ₄ N ₂ O ₄ S | 211.989 Da | Level 5 | – | – |
| P-W nu2 | – | C ₁₇ H ₃₂ N ₂ O ₈ | 392.2155 Da | Level 5 | – | – |
| P-W nu3 | – | C ₃₅ H ₆₀ N ₄ O ₁₃ | 744.4185 Da | Level 5 | – | – |
| P-W nd1 | – | C ₄₆ H ₇₅ N ₄ O ₁₆ P | 970.4906 Da | Level 5 | – | – |
| P-W nd2 | – | C ₂₆ H ₄₆ N ₆ O ₉ | 586.3324 Da | Level 5 | – | – |
| P-W nd3 | 65099 | C ₂₇ H ₅₀ O ₇ P ₂ | 548.3044 Da | Level 4 | – | – |

HPW group, but the differences were not statistically significant, whereas there were statistically significant differences between the GDM and HPW groups. Since isoleucine cannot be synthesized endogenously, and needs to be absorbed exogenously, the above-mentioned results indicate that the absorption of isoleucine was obviously reduced in pregnant women with GDM compared to HPW. In terms of differential metabolic pathways involving L-isoleucine between the GDM and HPW groups, we found that except for the shared differential metabolic pathways, ABC transporters; Valine, leucine, and isoleucine biosynthesis; and mineral absorption were differential metabolic pathways between the two groups. A previous study has shown that the ABC transporter family is associated with the development and progression of diabetes, dietary isoleucine can be absorbed through the intestine to bypass the hepatic first pass effect (Mann et al., 2021), while the P-glycoprotein (P-gp) encoded by the ABCB1 gene is mainly distributed in specific tissues such as the intestine, kidney, liver, and cerebrovascular endothelium, and the function and expression of P-GP are altered under diabetic conditions (Liu et al., 2006; Liu et al., 2007; Liu et al., 2008). Meanwhile, ABCC8 and ABCC9 are important components of ATP-sensitive potassium (KATP) channels, which can regulate KATP channel activity, and modulate insulin release to control blood glucose levels (Aguilar-Bryan and Bryan, 1999; Bryan et al., 2007). Therefore, we speculate that the changes in isoleucine level in patients with GDM may be caused by changes in P-gp, ABCC8, and ABCC9 expression.

Numerous studies (Doi et al., 2005; Doi et al., 2007; Ikehara et al., 2008; Guasch-Ferré et al., 2016; Ullrich et al., 2016; Newmire et al., 2019; Elovaris et al., 2021a; Elovaris et al., 2021b) have suggested that the effect of isoleucine on glucose metabolism may be related to the decreased expression of glucose-6-phosphatase (G6Pase). In the present study, we found that glucose 6-phosphate (G6P) level was elevated after pregnancy, presumably due to a decrease in G6Pase expression. Additionally, we found that except for the shared differential metabolic pathways involving D-glucose 6-phosphate, two pathways, namely, inositol phosphate metabolism and carbohydrate digestion and absorption, differed significantly between the GDM and HNPW groups. However, the changes in these two differential metabolic pathways did not result in a significant difference in changes in G6P level between the GDM and HPW groups. From these results, we hypothesize that changes in isoleucine expression, either upregulation or downregulation, can

both lead to a decrease in G6Pase expression. These results are similar to the findings from the previous studies investigating the alterations of isoleucine in diabetes.

Insulin resistance is a predominant pathogenic component of GDM. Several population studies have found that GDM can cause changes in maternal fatty acid metabolism, especially polyunsaturated fatty acids (PUFAs), during the third trimester of pregnancy (Wijendran et al., 1999; Thomas et al., 2004; Chen et al., 2010). PUFAs can be classified into n-3 PUFA [mainly derived from eicosapentaenoic acid (EPA), docosahexaenoic acid (DHA), and α -linolenic acid (ALA)] and n-6 PUFA [mainly derived from linoleic acid (LA) and arachidonic acid (AA)]. ALA is a dietary precursor for EPA and DHA (Gogus and Smith, 2010) and exerts anti-inflammatory and immunomodulatory effects mainly through regulation of cell proliferation and response activity, production of inflammatory cytokines, and adhesion molecule expression (Ho et al., 2011; Wutzler et al., 2013; Liu et al., 2015). LA, a precursor in the synthesis of AA, can increase the risk of chronic diseases via regulating inflammatory responses (Simopoulos, 2003; Yary et al., 2016).

The synthesis of other long-chain polyunsaturated fatty acids (LC-PUFAs) of the same series requires the enzyme systems such as fatty acid desaturases and elongase enzymes. The n-3 and n-6 PUFA synthesis share the same set of enzymes, resulting in the occurrence of competitive inhibition (Mariamenatu and Abdu, 2021). The mechanism linking the ratio of n-6 and n-3 PUFAs and diabetes has not yet been clarified. One explanation is that n-3 and n-6 PUFAs compete for desaturase and elongase enzymes, and conversion of LA to AA and ALA to DHA and EPA occurs through desaturation and elongation by δ -6 and δ -5 desaturases (Mozaffarian et al., 2005). ALA and its metabolites can inhibit the conversion of LA to AA, thus reducing the production of inflammatory markers (Pischoon et al., 2003). However, a higher intake of ALA may affect the pathway of n-6 PUFA metabolism. PUFAs can be transported from the mother to the fetus through the placenta (Makrides et al., 1994; Salem et al., 1996; Greiner et al., 1997), and the placenta preferentially takes up and transports fatty acids essential for fetal growth and development (Haggarty et al., 1997; Haggarty et al., 1999), with the order of preference being AA > DHA > ALA > LA (Haggarty, 2002).

GDM causes metabolic disorders involving fatty acids in maternal and cord blood, but fatty acid alterations display different trends in different tissues; for example, DHA levels are

TABLE 9 Enrichment of metabolic pathways of differential metabolites with identification confidence levels 1 and 2 between different groups.

| Group | Model | Location | Name | Level | KEGG ID | Pathway ID | Family | Metabolites |
|--------------|-------|--------------|----------------------------|---------|---------|---|-------------------------|---------------------------------|
| GDM vs. HPW | Pos | Down 54/77 | L-isoleucine | Level 1 | C00407 | map01100 Metabolic pathways map02010 ABC transporters map00290 Valine, leucine, and isoleucine biosynthesis map04978 Mineral absorption | Amino acids | Compounds with biological roles |
| | | Down 66/77 | Hypoxanthine | Level 1 | C00262 | map01100 Metabolic pathways | Purines and derivatives | Compounds with biological roles |
| | Neg | Down 8/20 | Docosahexaenoic acid | Level 2 | C06429 | map01040 Biosynthesis of unsaturated fatty acids | Fatty acyls | Lipids |
| | | Down 14/20 | Xanthine | Level 1 | C00385 | map00230 Purine metabolism map00232 Caffeine metabolism | Purines and derivatives | Compounds with biological roles |
| GDM vs. HNPW | Pos | Up 7/402 | Adenosine | Level 2 | C00212 | map00230 Purine metabolism map01100 Metabolic pathways map04024 cAMP signaling pathway map04080 Neuroactive ligand–receptor interaction map04270 Vascular smooth muscle contraction map04923 Regulation of lipolysis in adipocytes map05012 Parkinson disease map05032 Morphine addiction map05034 Alcoholism | Purines and derivatives | Compounds with biological roles |
| | | Down 213/421 | Retinoate | Level 2 | C00777 | map01100 Metabolic pathways map04659 Th17 cell differentiation map04672 Intestinal immune network for IgA production map05200 Pathways in cancer map05222 Small cell lung cancer map05223 Non-small cell lung cancer map05226 Gastric cancer | Prenol lipids | Lipids |
| | | Down 271/421 | Arachidonic acid | Level 2 | C00219 | map00591 Linoleic acid metabolism map01100 Metabolic pathways map04270 Vascular smooth muscle contraction map04726 Serotonergic synapse map04750 Inflammatory mediator regulation of TRP channels map04912 GnRH signaling pathway map04923 Regulation of lipolysis in adipocytes map05140 Leishmaniasis | Fatty acyls | Lipids |
| | Neg | Up 7/167 | Adenosine 5'-monophosphate | Level 2 | C00020 | map00230 Purine metabolism map01100 Metabolic pathways map01523 Antifolate resistance map04022 cGMP-PKG signaling pathway map04068 FoxO signaling pathway map04150 mTOR signaling pathway map04151 PI3K-Akt signaling pathway map04152 AMPK signaling pathway map04211 Longevity regulating pathway map04740 Olfactory transduction map04742 Taste transduction map04923 Regulation of lipolysis in adipocytes map04924 Renin secretion map04925 Aldosterone synthesis and secretion map04927 Cortisol synthesis and secretion map04928 Parathyroid hormone synthesis, | Purines and derivatives | Compounds with biological roles |

(Continued)

TABLE 9 Continued

| Group | Model | Location | Name | Level | KEGG ID | Pathway ID | Family | Metabolites |
|--------------|-------|------------------|--|------------|---------|--|--------------------------|---------------------------------|
| | | | | | | secretion and action map04934 Cushing syndrome map05012 Parkinson disease map05032 Morphine addiction | | |
| | | Up 117/ 167 | D-glucose 6-phosphate | Level 2 | C00092 | map00562 Inositol phosphate metabolism map01100 Metabolic pathways map04911 Insulin secretion map04917 Prolactin signaling pathway map04918 Thyroid hormone synthesis map04931 Insulin resistance map04973 Carbohydrate digestion and absorption | Carbohydrates | Compounds with biological roles |
| | | Down 174/ 174 | 8(s)-hydroxy-(5z,9e,11z,14z)-eicosatetraenoic acid | Level 2 | C14776 | map00590 Arachidonic acid metabolism map01100 Metabolic pathways map03320 PPAR signaling pathway | Fatty acyls | Lipids |
| HPW vs. HNPW | Pos | Up 189/ 351 | Adenosine-monophosphate | Level 1 | C00020 | map00230 Purine metabolism map01100 Metabolic pathways map01523 Antifolate resistance map04068 FoxO signaling pathway map04150 mTOR signaling pathway map04151 PI3K-Akt signaling pathway map04923 Regulation of lipolysis in adipocytes map04925 Aldosterone synthesis and secretion map04927 Cortisol synthesis and secretion map04934 Cushing syndrome | Nucleic acids | Compounds with biological roles |
| | | Up 192/ 351 | L-(–)-methionine | Level 2 | C00073 | map00970 Aminoacyl-tRNA biosynthesis map01100 Metabolic pathways map01523 Antifolate resistance map04974 Protein digestion and absorption map04978 Mineral absorption | Amino acids | Compounds with biological roles |
| | | Up 235/ 351 | Cortisol | Level 2 | C00735 | map01100 Metabolic pathways map04927 Cortisol synthesis and secretion map04934 Cushing syndrome map04976 Bile secretion | Steroids and derivatives | Compounds with biological roles |
| | | Down 93/ 296 | Arachidonic acid | Level 2 | C00219 | map00591 Linoleic acid metabolism map01100 Metabolic pathways map04726 Serotonergic synapse map04912 GnRH signaling pathway map04923 Regulation of lipolysis in adipocytes map04925 Aldosterone synthesis and secretion map05140 Leishmaniasis | Fatty acyls | Lipids |
| | Neg | Up 9/112 | Adenosine 5'-monophosphate | Level 2 | C00020 | map00230 Purine metabolism map01100 Metabolic pathways map01523 Antifolate resistance map04022 cGMP-PKG signaling pathway map04024 cAMP signaling pathway map04068 FoxO signaling pathway map04150 mTOR signaling pathway map04151 PI3K-Akt signaling pathway map04152 AMPK signaling pathway map04211 Longevity regulating pathway map04740 Olfactory transduction map04742 Taste transduction map04923 Regulation of lipolysis in adipocytes map04924 Renin secretion map04925 Aldosterone synthesis and | Purines and derivatives | Compounds with biological roles |

(Continued)

TABLE 9 Continued

| Group | Model | Location | Name | Level | KEGG ID | Pathway ID | Family | Metabolites |
|-------|-------|-----------|-----------------------|---------|---------|--|---------------|---------------------------------|
| | | | | | | secretion map04927 Cortisol synthesis and secretion map04928 Parathyroid hormone synthesis, secretion and action map04934 Cushing syndrome map05012 Parkinson disease map05032 Morphine addiction | | |
| | | Up 93/112 | D-glucose 6-phosphate | Level 2 | C00092 | map01100 Metabolic pathways map04911 Insulin secretion map04917 Prolactin signaling pathway map04918 Thyroid hormone synthesis map04931 Insulin resistance | Carbohydrates | Compounds with biological roles |

markedly higher in the serum or plasma and lower in the erythrocyte membranes of patients with GDM; these differences in AA and DHA levels in the serum/plasma and the erythrocyte membranes may be related to the negative feedback regulation of the human body. The plasma fatty acids reflect short-term fatty acid intake (1 to 2 weeks), and the plasma fatty acid levels are influenced by many factors, such as the physiological state of the body, dietary intake, and genes, whereas the erythrocyte fatty acid levels can accurately reflect the long-term (approximately 1 to 2 months) dietary fatty acid intake (Hai-Tao et al., 2021).

The results of this study showed that DHA expression was significantly downregulated in the GDM group compared with the HPW group. Meanwhile, DHA expression was significantly downregulated in the GDM group compared with the HNPW group, whereas no statistically significant difference was found between the HPW and HNPW groups. DHA was annotated to biosynthesis of unsaturated fatty acids (map01040) pathway. Compared with the HNPW group, AA levels was significantly downregulated in both the GDM and HPW groups, but no statistically significant difference was found between GDM and HPW groups. In terms of differential metabolic pathways involving AA, changes in AA expression in two pathways including vascular smooth muscle contraction map (map04270) and inflammatory mediator regulation of TRP channels (map04750) were observed in the GDM group when compared with the HNPW group. Unlike the GDM group, changes in AA expression were observed in aldosterone synthesis and secretion (map04925) pathway in the HPW group when compared with the HNPW group.

We speculate that the possible reasons for the downregulation of DHA in the GDM group are as follows: (i) the lack of precursor substances for DHA synthesis due to inadequate ALA intake from foods in GDM patients; (ii) although adequate ALA intake from foods is achieved, the synthesis of AA is stronger than that of DHA due to the presence of insulin resistance and the competition between n-3 and n-6 PUFAs. According to the differential metabolic pathways involving AA observed in this study, we suggest that when GDM occurs, AA is involved in the chronic inflammatory response, and has an impact on the placental transport of maternal PUFAs.

Under normal physiological conditions, the ratio of adenosine monophosphate (AMP), adenosine bisphosphonate (ADP), and

adenosine triphosphate (ATP) is in a relatively stable state. However, under excessive starvation, ischemic conditions, or other extreme conditions, the production of ATP is insufficient, ADP accumulation occurs, and the lack of ATP is compensated to some extent through the reaction $2ADP \rightarrow ATP + AMP$, resulting in an increase in AMP levels. Since the AMP/ATP ratio varies as the square of the ADP/ATP ratio (Hardie and Hawley, 2001), sensing the levels of AMP is more sensitive than ADP.

When AMP content is high with low energy, the phosphorylation of AMP-activated protein kinase (AMPK) by the upstream kinases is promoted, thus increasing AMPK activity (Hawley et al., 1995; Xiao et al., 2007). Allosteric activation of AMPK induced by AMP further results in a two- to threefold increase in AMPK activity after phosphorylation, the increase varies with ATP levels (Gowans et al., 2013), and maximum AMPK activation can be reached (Sanders et al., 2007). AMP and ADP binding also inhibits AMPK dephosphorylation mediated by phosphatases (Davies et al., 1995; Xiao et al., 2011), and the binding of AMPK complexes to ADP or AMP also leads to conformational changes, thus promoting phosphorylation of a threonine residue (Thr-172) and inhibiting its dephosphorylation. AMPK activation can improve insulin sensitivity and glucose homeostasis, and AMPK inactivation is associated with various metabolic disorders, reflecting its importance as a therapeutic target (Cabarcas et al., 2010).

AMP is an important regulator of insulin and Akt protein kinase signaling pathways. It has been shown that Akt could regulate the inhibitory effect of insulin on AMPK (Kovacic et al., 2003). Akt cannot directly phosphorylate AMPK. Insulin-induced changes in Akt activity can regulate AMPK activity by altering the intracellular AMP/ATP ratio. In fact, the activation of Akt could reduce the intracellular AMP/ATP ratio, leading to a decrease in AMPK activity (Hahn-Windgassen et al., 2005). Therefore, the insulin–Akt signaling axis can expand the range of metabolic effects by upregulating AMP signaling and increasing AMPK activity.

The results of the present study showed that compared with the HNPW group, the expression of adenosine and adenosine 5'-monophosphate was significantly upregulated in the GDM group, and the expression of adenosine-monophosphate and adenosine 5'-monophosphate was significantly upregulated in the HPW group, but the difference was not significant between the GDM and HPW

groups. In terms of the annotated differential metabolic pathways, except for the cAMP signaling pathway involving adenosine 5'-monophosphate that was determined in the HPW group when compared with the HNPW group, differential metabolic pathways of the GDM and HNPW groups compared with the HNPW group were the same. This also seems to indicate that that, after pregnancy, the energy requirements of pregnant women increase, and the AMPK activity changes accordingly, so it is speculated that insulin sensitivity and glucose homeostasis in GDM patients may be affected if the changes in AMPK activity are insufficient to meet the body's needs.

GDM and type 2 diabetes mellitus have similar precipitating factors leading to glucose metabolism disorders. Uric acid has been suggested to possibly affect oxidative stress, inflammatory responses, and enzymes associated with glucose and lipid metabolic homeostasis (Lima et al., 2015). The results of this study showed that uric acid expression was significantly upregulated in both the GDM and HPW groups compared with the HNPW group, whereas no statistically significant difference was found between the GDM and HPW groups. However, the expression of uric acid precursors, anthine and hypoxanthine, was significantly downregulated in the GDM group compared with the PWM group; there was no statistically significant difference between the GDM and HNPW groups. In terms of differential metabolic pathways involving anthine and hypoxanthine among GDM and HPW groups, xanthine was annotated to two pathways, purine metabolism (map00230) and caffeine metabolism (map00232), and hypoxanthine was only annotated to metabolic pathways (map01100), but the next level of pathways is not yet known.

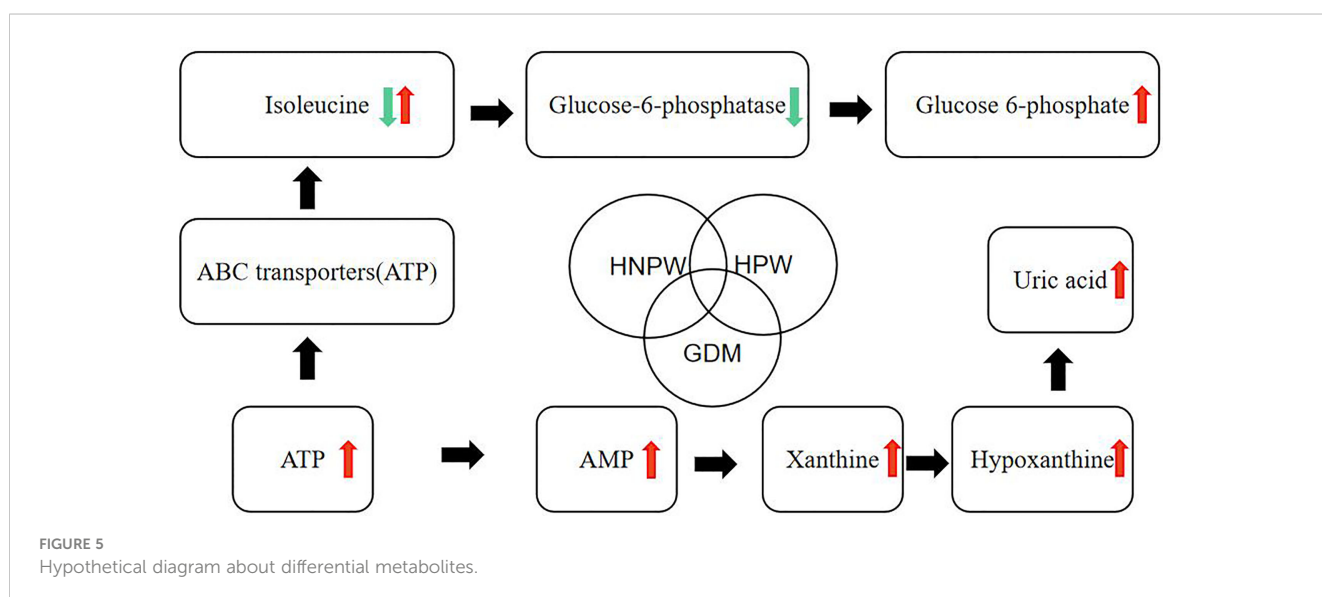
At present, according to findings from previously published studies on the relationship between serum uric acid levels and GDM, some scholars suggest that uric acid levels were positively correlated with the risk of GDM (Kharb, 2008; Laughon et al., 2009; Wolak et al., 2010; Wang, 2012; Gkiomisi et al., 2013; Rasika et al., 2014; Aker et al., 2016; Amudha et al., 2017), while some studies documented that there was no significant difference in the uric acid levels between patients with GDM and healthy controls (Seghieri

et al., 2003; Güngör et al., 2006; Davari-Tanha et al., 2008; Maged et al., 2014), and some even suggest that serum uric acid levels were significantly lower in the GDM group than in the non-GDM group (Javadian et al., 2014). The results of a meta-analysis conducted by Zhao support a correlation between uric acid levels and the incidence of GDM (Diqi, 2018).

Xanthine oxidoreductase (XOR) has two redox isoforms, xanthine dehydrogenase (XDH) and xanthine oxidase (XO), which is mainly found in capillary endothelial cells, and these two forms are interconvertible (Battelli et al., 2014). Under normal physiological conditions, it mainly exists in the form of XDH. During ischemia and hypoxia, the synthesis of XDH increases due to the decrease of ATP production and the dysfunction of membrane pump, which is converted to large amounts of XO. At the same time, ATP cannot be used to release energy, and is degraded to ADP, AMP, and hypoxanthine, leading to large accumulation of hypoxanthine in the ischemic tissues. During reperfusion, a large amount of molecular oxygen enters into the ischemic tissues along with the blood, XO catalyzes the conversion of hypoxanthine to xanthine again, and further catalyzes the conversion of xanthine to uric acid. These processes use molecular oxygen as an electron acceptor, resulting in the production of a large amount of superoxide anion and hydrogen peroxide (Nørholt et al., 1996; Chen et al., 2004), which can cause hypoxic tissue damage directly, and the body may also enter a state of oxidative stress, leading to vascular endothelial damage and promoting the progression of GDM.

Based on the findings of the above-mentioned previous studies and results of the present study, we hypothesized that the elevated expression of xanthine and hypoxanthine in the HPW group may be due to the relatively lower degree of hypoxia in the HPW group compared to the GDM group; this leads to a decrease in the production or activity of XO, thereby decreasing the synthesis of uric acid. Additionally, the oxygen demand is higher in patients with GDM than in HPW.

In this study, we made a hypothetical map (Figure 5) of several metabolites that were found to be different in the comparison of



GDM, HPW, and HNPW, so as to further elaborate and confirm their correlation in subsequent studies.

5 Conclusion

In conclusion, untargeted metabolomic analysis of saliva samples from pregnant women with DGM, HPW, and HNPW identified nine differential metabolites with high confidence. The results are similar to findings from previous metabolomics studies of serum and urine samples, which offer the possibility of using saliva for regular noninvasive testing in the population of pregnant women with and without GDM. Meanwhile, the associations between these identified differential metabolites and gingivitis need to be further validated by subsequent studies.

Data availability statement

The data presented in the study are deposited in the MetaboLights database repository, accession number MTBLS7774.

Ethics statement

The studies involving human participants were reviewed and approved by The Research Ethics Committee of Stomatological Hospital of Chongqing Medical University. The patients/participants provided their written informed consent to participate in this study.

Author contributions

YL, YF, and ZY conceived the research theme and supervised the entire study. YL collected the data, analyzed the data, drew the figures, explained the results, and drafted the manuscript. DJ, JL,

and ZZ revised the manuscript and performed reference collection. All authors contributed to the article and approved the submitted version.

Funding

This work was supported by the Chongqing Municipal Health Commission (No. 2021MSXM312 and No. 2021MSXM290) and the First Batch of Key Disciplines on Public Health in Chongqing. The funders had no role in study design, data collection and analysis, decision to publish, or preparation of the manuscript.

Acknowledgments

We thank BGI Tech Solutions Co., Ltd for technical assistance with mass spectrometry analysis work (LC-MS/MS). We would like to thank all the contributors in this study.

Conflict of interest

The authors declare that the research was conducted in the absence of any commercial or financial relationships that could be construed as a potential conflict of interest.

Publisher's note

All claims expressed in this article are solely those of the authors and do not necessarily represent those of their affiliated organizations, or those of the publisher, the editors and the reviewers. Any product that may be evaluated in this article, or claim that may be made by its manufacturer, is not guaranteed or endorsed by the publisher.

References

- Aguilar-Bryan, L., and Bryan, J. (1999). Molecular biology of adenosine triphosphate-sensitive potassium channels. *Endocr. Rev.* 20 (2), 101–135. doi: 10.1210/edrv.20.2.0361
- Aker, S. Ş, Yüce, T., Kalafat, E., Seval, M., and Söylemez, F. (2016). Association of first trimester serum uric acid levels gestational diabetes mellitus development. *Turk J. Obstet. Gynecol.* 13 (2), 71–74. doi: 10.4274/tjod.69376
- Amudha, P., Nithya, D., Pradeeba, S., and Manochithra, B. (2017). Correlation between first trimester uric acid level and subsequent development of gestational diabetes mellitus. *IJRCOG.* 6 (2), 606. doi: 10.18203/2320-1770.ijrcog20170391
- Barker, M., and Rayens, W. (2003). Partial least squares for discrimination. *J. Chemometr.* 17 (3), 166–173. doi: 10.1002/cem.785
- Battelli, M. G., Bolognesi, A., and Polito, L. (2014). Pathophysiology of circulating xanthine oxidoreductase: new emerging roles for a multi-tasking enzyme. *Biochim. Biophys. Acta* 1842 (9), 1502–1517.
- Bryan, J., Muñoz, A., Zhang, X., Düfer, M., Drews, G., Krippeit-Drews, P., et al. (2007). ABC8 and ABC9: ABC transporters that regulate k⁺ channels. *Pflugers Arch.* 453 (5), 703–718. doi: 10.1007/s00424-006-0116-z
- Cabarcas, S. M., Hurt, E. M., and Farrar, W. L. (2010). Defining the molecular nexus of cancer, type 2 diabetes and cardiovascular disease. *Curr. Mol. Med.* 10 (8), 744–755. doi: 10.2174/156652410793384187
- Chen, X., Scholl, T. O., Leskiw, M., Savaille, J., and Stein, T. P. (2010). Differences in maternal circulating fatty acid composition and dietary fat intake in women with gestational diabetes mellitus or mild gestational hyperglycemia. *Diabetes Care* 33 (9), 2049–2054. doi: 10.2337/dc10-0693
- Chen, P. H., Wu, W. L., Liu, Z. H., and Gao, C. R. (2004). Tramadol or lornoxicam reduces restlessness during recovery after general anesthesia. *China J. Modern Med.* 14 (6), 129–131.
- Cheng, X. Q., Deng, M., Xu, X., and Zhou, X. D. (2014). Saliva and salivaomics in early diagnosis of diseases. *Guoji Kou Qiang Yi Xue Za Zhi* 41 (2), 213–219.
- Cheng, X. Q., Zhou, X. D., and Xu, X. (2016). Application of saliva in disease diagnosis. *Hua Xi Kou Qiang Yi Xue Za Zhi* 34 (6), 647–653.
- Davari-Tanha, F., Khan-Mohamadi, F., Kaveh, M., Shariat, M., and Kochak, M. (2008). Homocysteine in gestational diabetes and normal pregnancy plus effects of folic acid. *Iranian J. Public Health* 37 (3), 118–126.

- Davies, S. P., Helps, N. R., Cohen, P. T., and Hardie, D. G. (1995). 5'-AMP inhibits dephosphorylation, as well as promoting phosphorylation, of the AMP-activated protein kinase. Studies using bacterially expressed human protein phosphatase-2C α and native bovine protein phosphatase-2A α . *FEBS Lett.* 377 (3), 421–425. doi: 10.1016/0014-5793(95)01368-7
- Diqi, Z. (2018). A meta-analysis of serum uric acid levels in pregnant with gestational diabetes and non-gestational diabetes. *Chongqing:Chong Qing Med. University* 19.
- Doi, M., Yamaoka, I., Nakayama, M., Mochizuki, S., Sugahara, K., Yoshizawa, F., et al. (2005). Isoleucine, a blood glucose-lowering amino acid, increases glucose uptake in rat skeletal muscle in the absence of increases in AMP-activated protein kinase activity. *J. Nutr.* 135 (9), 2103–2108. doi: 10.1093/jn/135.9.2103
- Doi, M., Yamaoka, I., Nakayama, M., Sugahara, K., and Yoshizawa, F. (2007). Hypoglycemic effect of isoleucine involves increased muscle glucose uptake and whole body glucose oxidation and decreased hepatic gluconeogenesis. *Am. J. Physiol. Endocrinol. Metab.* 292 (6), E1683–E1693. doi: 10.1152/ajpendo.00609.2006
- Domisch, H., Staufenbiel, L., Schulze, K., Stiesch, M., Winkel, A., Fimmers, R., et al. (2015). Expression of antimicrobial peptides and interleukin-8 during early stages of inflammation: an experimental gingivitis study. *J. Periodontol. Res.* 50 (6), 836–845. doi: 10.1111/jre.12271
- Elovaris, R. A., Bitarafan, V., Agah, S., Ullrich, S. S., Lange, K., Horowitz, M., et al. (2021a). Comparative effects of the branched-chain amino acids, leucine, isoleucine and valine, on gastric emptying, plasma glucose, c-peptide and glucagon in healthy men. *Nutrients* 13 (5), 1613. doi: 10.3390/nu13051613
- Elovaris, R. A., Hajishafiee, M., Ullrich, S. S., Fitzgerald, P. C. E., Lange, K., Horowitz, M., et al. (2021b). Intra-gastric administration of leucine and isoleucine does not reduce the glycaemic response to, or slow gastric emptying of, a carbohydrate-containing drink in type 2 diabetes. *Diabetes Res. Clin. Pract.* 171, 108618. doi: 10.1016/j.diabres.2020.108618
- Gkiomisi, A., Makedou, K. G., Anastasilakis, A. D., Polyzos, S. A., Kourtis, A., Gerou, S., et al. (2013). Serum vaspin levels in women with and without gestational diabetes mellitus during pregnancy and postpartum. *Cytokine* 61 (1), 127–132. doi: 10.1016/j.cyto.2012.09.006
- Gogus, U., and Smith, C. (2010). Omega 3 fatty acids: a review of current knowledge. *Int. J. Food Sci. Technol.* 45 (4), 417–436. doi: 10.1111/j.1365-2621.2009.02151.x
- Goldsmith, P., Fenton, H., Morris-Stiff, G., Ahmad, N., Fisher, J., and Prasad, K. R. (2010). Metabonomics: a useful tool for the future surgeon. *J. Surg. Res.* 160 (1), 122–132. doi: 10.1016/j.jss.2009.03.003
- Gowans, G. J., Hawley, S. A., Ross, F. A., and Hardie, D. G. (2013). AMP is a true physiological regulator of AMP-activated protein kinase by both allosteric activation and enhancing net phosphorylation. *Cell Metab.* 18 (4), 556–566. doi: 10.1016/j.cmet.2013.08.019
- Greiner, R. C., Winter, J., Nathanielsz, P. W., and Brenna, J. T. (1997). Brain docosahexaenoate accretion in fetal baboons: bioequivalence of dietary α -linolenic and docosahexaenoic acids. *Pediatr. Res.* 42 (6), 826–834. doi: 10.1203/00006450-199712000-00018
- Guasch-Ferré, M., Hruby, A., Toledo, E., Clish, C. B., Martínez-González, M. A., Salas-Salvadó, J., et al. (2016). Metabonomics in prediabetes and diabetes: a systematic review and meta-analysis. *Diabetes Care* 39 (5), 833–846. doi: 10.2337/dci15-2251
- Güngör, E. S., Danişman, N., and Mollamahmutoglu, L. (2006). Relationship between serum uric acid, creatinine, albumin and gestational diabetes mellitus. *Clin. Chem. Lab. Med.* 61 (8), 974–977.
- Haackel, R., and Hnecke, P. (1993). The application of saliva, sweat and tear fluid for diagnostic purposes. *Annales DeBiologie Clinique* 51 (10-11), 903.
- Haggarty, P. (2002). Placental regulation of fatty acid delivery and its effect on fetal growth - a review. *Placenta* 23, S28–S38. doi: 10.1053/plac.2002.0791
- Haggarty, P., Ashton, J., Joynson, M., Abramovich, D. R., and Page, K. (1999). Effect of maternal polyunsaturated fatty acid concentration on transport by the human placenta. *Biol. Neonate* 75 (6), 350–359. doi: 10.1159/000014115
- Haggarty, P., Page, K., Abramovich, D. R., Ashton, J., and Brown, D. (1997). Long-chain polyunsaturated fatty acid transport across the perfused human placenta. *Placenta* 18 (8), 635–642. doi: 10.1016/s0143-4004(97)90004-7
- Hahn-Windgassen, A., Nogueira, V., Chen, C.-C., Skeen, J. E., Sonenberg, N., and Hay, N. (2005). Akt activates the mammalian target of rapamycin by regulating cellular ATP level and AMPK activity. *J. Biol. Chem.* 280 (37), 32081–32089. doi: 10.1074/jbc.M502876200
- Hai-Tao, Y., Zhi-Heng, G., Yi-Ru, C., Yue-Ting, L., Hai-Ying, Z., Ya-Juan, L., et al. (2021). Gestational diabetes mellitus decreased umbilical cord blood polyunsaturated fatty acids: a meta-analysis of observational studies. *Prostaglandins Leukotrienes Essential Fatty Acids* 171, 102318. doi: 10.1016/j.plfa.2021.102318
- Hardie, D. G., and Hawley, S. A. (2001). AMP-activated protein kinase: the energy charge hypothesis revisited. *BioEssays* 23 (12), 1112–1119. doi: 10.1002/bies.10009
- Hawley, S. A., Selbert, M. A., Goldstein, E. G., Edelman, A. M., Carling, D., and Hardie, D. G. (1995). 5'-AMP activates the AMP-activated protein kinase cascade, and Ca²⁺/calmodulin activates the calmodulin-dependent protein kinase I cascade, via three independent mechanisms. *J. Biol. Chem.* 270 (45), 27186–27191. doi: 10.1074/jbc.270.45.27186
- Ho, Y. P., Chiu, C. T., Sheen, I. S., Tseng, S. C., Lai, P. C., Ho, S. Y., et al. (2011). Tumor necrosis factor- α and interleukin-10 contribute to immunoparalysis in patients with acute pancreatitis. *Hum. Immunol.* 72 (1), 18–23. doi: 10.1016/j.humimm.2010.10.002
- Hu, C. Z., Guo, J. J., Yang, Y. Z., Wang, B., Tao, Q., Zhou, X. Y., et al. (1999). Investigation and analysis of pregnancy gingivitis in 700 pregnancy women. *Shanghai J. Stomatol* 8 (1), 1517.
- Ikehara, O., Kawasaki, N., Maezono, K., Komatsu, M., and Konishi, A. (2008). Acute and chronic treatment of l-isoleucine ameliorates glucose metabolism in glucose-intolerant and diabetic mice. *Biol. Pharm. Bull.* 31 (3), 469–472. doi: 10.1248/bpb.31.469
- Javadian, P., Alimohamadi, S., Gharedaghi, M. H., and Hantoushzadeh, S. (2014). Gestational diabetes mellitus and iron supplement; effects on pregnancy outcome. *Acta Med. Iran* 52 (5), 385–389.
- Jusko, W. J., and Milsap, R. L. (1993). Pharmacokinetic principles of drug distribution in saliva. *Ann. N. Y. Acad. Sci.* 694, 36. doi: 10.1111/j.1749-6632.1993.tb18340.x
- Kharb, S. (2008). Total radical-trapping antioxidant potential in gestational diabetes. *Int. J. Gynaecol. Obstet.* 103 (3), 257–258. doi: 10.1016/j.ijgo.2008.06.017
- Komine-Aizawa, S., Aizawa, S., and Hayakawa, S. (2019). Periodontal diseases and adverse pregnancy outcomes. *J. Obstet. Gynaecol. Res.* 45 (1), 5–12. doi: 10.1111/jog.13782
- Kovacic, S., Soltys, C.-L. M., Barr, A. J., Shiojima, I., Walsh, K., Dyck, J. R., et al. (2003). Akt activity negatively regulates phosphorylation of AMP-activated protein kinase in the heart. *J. Biol. Chem.* 278 (41), 39422–39427. doi: 10.1074/jbc.M305371200
- Laughon, S. K., Catov, J., Provins, T., Roberts, J. M., and Gandy, R. E. (2009). Elevated first-trimester uric acid concentrations are associated with the development of gestational diabetes. *Am. J. Obstet Gynecol* 201 (4), 1–5. doi: 10.1016/j.ajog.2009.06.065
- Liang, L., Rasmussen, M. L., Piening, B., Shen, X., Chen, S., Röst, H., et al. (2020). Metabolic dynamics and prediction of gestational age and time to delivery in pregnant women. *Cell* 181 (7), 1680–1692. doi: 10.1016/j.cell.2020.05.002
- Lima, W. G., Martins-Santos, M. E., and Chaves, V. E. (2015). Uric acid as a modulator of glucose and lipid metabolism. *Biochimie* 116, 17–23. doi: 10.1016/j.biochi.2015.06.025
- Liu, Y. H., Li, X. Y., Chen, C. Y., Zhang, H. M., and Kang, J. X. (2015). Omega-3 fatty acid intervention suppresses lipopolysaccharide-induced inflammation and weight loss in mice. *Mar. Drugs* 13 (2), 1026–1036. doi: 10.3390/md13021026
- Liu, H., Liu, X., Jia, L., Liu, Y., Yang, H., Wang, G., et al. (2008). Insulin therapy restores im-paired function and expression of p-glycoprotein in blood-brain barrier of experimental diabetes. *Biochem. Pharmacol.* 75 (8), 1649–1658. doi: 10.1016/j.bcp.2008.01.004
- Liu, H., Xu, X., Yang, Z., Deng, Y., Liu, X., and Xie, L. (2006). Impaired function and expression of p-glycoprotein in blood-brain barrier of streptozotocin-induced diabetic rats. *Brain Res.* 1123 (1), 245–252. doi: 10.1016/j.brainres.2006.09.061
- Liu, H., Zhang, D., Xu, X., Liu, X., Wang, G., Xie, L., et al. (2007). Attenuated function and expression of p-glycoprotein at blood-brain barrier and increased brain distribution of phenobarbital in streptozotocin-induced diabetic mice. *Eur J Pharmacol.* 561 (123), 226–232. doi: 10.1016/j.ejphar.2007.01.062
- Maged, A. M., Moety, G. A., Mostafa, W. A., and Hamed, D. A. (2014). Comparative study between different biomarkers for early prediction of gestational diabetes mellitus. *J. Matern. Fetal Neonatal Med.* 27 (11), 1108–1112. doi: 10.3109/14767058.2013.850489
- Makrides, M., Neumann, M. A., Byard, R. W., Simmer, K., and Gibson, R. A. (1994). Fatty acid composition of brain, retina, and erythrocytes in breast- and formula-fed infants. *Am. J. Clin. Nutr.* 60 (2), 189–194. doi: 10.1093/ajcn/60.2.189
- Mann, G., Mora, S., Madu, G., and Adegoke, O. A. J. (2021). Branched-chain amino acids: catabolism in skeletal muscle and implications for muscle and whole-body metabolism. *Front. Physiol.* 12, 702826. doi: 10.3389/fphys.2021.702826
- Mariamnatu, A. H., and Abdu, E. M. (2021). Overconsumption of omega-6 polyunsaturated fatty acids (PUFAs) versus deficiency of omega-3 PUFAs in modern-day diets: the disturbing factor for their "Balanced antagonistic metabolic functions" in the human body. *J. Lipids* 2021, 8848161. doi: 10.1155/2021/8848161
- Mozaffarian, D., Ascherio, A., Hu, F. B., Stampfer, M. J., Willett, W. C., Siscovick, D. S., et al. (2005). Interplay between different polyunsaturated fatty acids and risk of coronary heart disease in men. *Circulation* 111 (2), 157–164. doi: 10.1161/01.CIR.0000152099.87287.83
- Newmire, D. E., Rivas, E., Deemer, S. E., Willoughby, D. S., and Ben-Ezra, V. (2019). The impact of a large bolus dose of l-leucine and l-isoleucine on enteroendocrine and pancreatic hormones, and glycemia in healthy, inactive adults. *Nutrients* 11 (11), 2650. doi: 10.3390/nu11112650
- Nørholt, S. E., Sindet-Pedersen, S., Larsen, U., Bang, U., Ingerslev, J., Nielsen, O., et al. (1996). Pain control after dental surgery: a double-blind, randomised trial of lornoxicam versus morphine. *Pain* 67 (2-3), 335–343. doi: 10.1016/0304-3959(96)03126-0
- Pischoon, T., Hankinson, S. E., Hotamisligil, G. S., Rifai, N., Willett, W. C., and Rimm, E. B. (2003). Habitual dietary intake of n-3 and n-6 fatty acids in relation to inflammatory markers among US men and women. *Circulation* 108 (2), 155–160. doi: 10.1161/01.CIR.0000079224.46084.C2
- Rasika, C., Samal, S., and Ghose, S. (2014). Association of elevated first trimester serum uric acid levels with development of GDM. *J. Clin. Diagn. Res.* 8 (12), 01–05. doi: 10.7860/JCDR/2014/8063.5226

- Rhodus, N. L., Cheng, B., Myers, S., Bowles, W., Ho, V., and Ondrey, F. (2005). A comparison of the pro-inflammatory, NF-kappa b- dependent cytokines: TNF- alpha, IL-1-alpha, IL-6, and IL- 8 in different oral fluids from oral lichen planus patients. *Clin. Immunol.* 114 (3), 278–283. doi: 10.1016/j.clim.2004.12.003
- Salem, N. Jr., Wegher, B., Mena, P., and Uauy, R. (1996). Arachidonic and docosahexaenoic acids are biosynthesized from their 18-carbon precursors in human infants. *Proc. Natl. Acad. Sci. U.S.A.* 93 (1), 49–54. doi: 10.1073/pnas.93.1.49
- Sanders, M. J., Grondin, P. O., Hegarty, B. D., Snowden, M. A., and Carling, D. (2007). Investigating the mechanism for AMP activation of the AMP-activated protein kinase cascade. *Biochem. J.* 403 (1), 139–148. doi: 10.1042/BJ20061520
- Seghieri, G., Breschi, M. C., Anichini, R., De Bellis, A., Alviggi, L., Maida, I., et al. (2003). Serum homocysteine levels are increased in women with gestational diabetes mellitus. *Metabolism* 52 (6), 720–723. doi: 10.1016/s0026-0495(03)00032-5
- Shen, B., Yi, X., Sun, Y., Bi, X., Du, J., Zhang, C., et al. (2020). Proteomic and metabolomic characterization of COVID-19 patient sera. *Cell* 182 (1), 59–72.
- Simopoulos, A. P. (2003). Essential fatty acids in health and chronic diseases. *Forum Nutr.* 56, 67–70.
- Thomas, B., Ghebremeskel, K., Lowy, C., Min, Y., and Crawford, M. A. (2004). Plasma AA and DHA levels are not compromised in newly diagnosed gestational diabetic women. *Eur. J. Clin. Nutr.* 58 (11), 1492–1497. doi: 10.1038/sj.ejcn.1601996
- Ullrich, S. S., Fitzgerald, P. C., Schober, G., Steinert, R. E., Horowitz, M., and Feinle-Bisset, C. (2016). Intra-gastric administration of leucine or isoleucine lowers the blood glucose response to a mixed-nutrient drink by different mechanisms in healthy, lean volunteers. *Am. J. Clin. Nutr.* 104 (5), 1274–1284. doi: 10.3945/ajcn.116.140640
- Wang, Z. (2012). Combination of lipids and uric acid in mid-second trimester can be used to predict adverse pregnancy outcomes. *J. Matern. Fetal Neonatal Med.* 25 (12), 2633.
- Wen, B., Mei, Z. L., Zeng, C., and Liu, S. (2017). metaX: a flexible and comprehensive software for processing metabolomics data. *BMC Bioinf.* 18 (1), 183. doi: 10.1186/s12859-017-1579-y
- Westerhuis, J. A., Hoefsloot, H. C. J., Smit, S., Vis, D. J., Smilde, A. K., Velzen, E. J. J. V., et al. (2008). Assessment of PLS-DA cross validation. *Metabolomics* 4 (1), 81–89. doi: 10.1007/s11306-007-0099-6
- Wijendran, V., Bendel, R. B., Couch, S. C., Philipson, E. H., Thomsen, K., Zhang, X., et al. (1999). Maternal plasma phospholipid polyunsaturated fatty acids in pregnancy with and without gestational diabetes mellitus. *Am. J. Clin. Nutr.* 70 (1), 53–61. doi: 10.1093/ajcn/70.1.53
- Wolak, T., Sergienko, R., Wiznitzer, A., Paran, E., and Sheiner, E. (2010). High uric acid level during the first 20 weeks of pregnancy is associated with higher risk for gestational diabetes mellitus and mild preeclampsia. *Hypertension Pregnancy* 31 (3), 307–315.
- Wu, M., Chen, S. W., and Jiang, S. Y. (2015). Relationship between gingival inflammation and pregnancy. *Mediator. Inflamm.* 2015, 623427. doi: 10.1155/2015/623427
- Wutzler, A., Kestler, C., Perrot, A., Loehr, L., Huemer, M., Parwani, A. S., et al. (2013). Variations in the human soluble epoxide hydrolase gene and recurrence of atrial fibrillation after catheter ablation. *Int. J. Cardiol.* 168 (4), 3647–3651.
- Xiao, B., Heath, R., Saiu, P., Leiper, F. C., Leone, P., Jing, C., et al. (2007). Structural basis for AMP binding to mammalian AMP-activated protein kinase. *Nature* 449 (7161), 496–500. doi: 10.1038/nature06161
- Xiao, B., Sanders, M. J., Underwood, E., Heath, R., Mayer, F. V., Carmena, D., et al. (2011). Structure of mammalian AMPK and its regulation by ADP. *Nature* 472 (7342), 230–233. doi: 10.1038/nature09932
- Xiong, X., Buekens, P., Vastardis, S., and Pridjian, G. (2006). Periodontal disease and gestational diabetes mellitus. *Am. J. Obstet. Gynecol.* 195 (4), 1086–1089. doi: 10.1016/j.ajog.2006.06.035
- Yary, T., Voutilainen, S., Tuomainen, T. P., Ruusunen, A., Nurmi, T., and Virtanen, J. K. (2016). Serum n-6 polyunsaturated fatty acids, Delta5- and Delta6-desaturase activities, and risk of incident type 2 diabetes in men: the kuopio ischaemic heart disease risk factor study. *Am. J. Clin. Nutr.* 103 (5), 1337–1343. doi: 10.3945/ajcn.115.128629
- Zhang, C. Z., Cheng, X. Q., Li, J. Y., Zhang, P., Yi, P., Xu, X., et al. (2016). Saliva in the diagnosis of diseases. *Int. J. Oral. Sci.* 8 (3), 133–137. doi: 10.1038/ijos.2016.38
- Zheng, W. B., Zou, Y., Elsheikha, H. M., Liu, G. H., Hu, M. H., Wang, S. L., et al. (2019). Serum metabolomic alterations in beagle dogs experimentally infected with *Toxocara canis*. *Parasit Vectors* 12 (1), 447. doi: 10.1186/s13071-019-3703-5